Charge transfer fluctuations as a signal for quark-gluon plasma

Lijun Shi*
Physics Department, McGill University, Montréal, Québec, H3A 2T8 Canada

Sangyong Jeon†
Physics Department, McGill University, Montréal, Québec, H3A 2T8 Canada and RIKEN-BNL Research Center, Upton, New York 11973, USA

(Received 18 March 2005; published 27 September 2005)

In this work, the charge transfer fluctuation that was previously used for *pp* collisions is proposed for relativistic heavy-ion collisions as a quark-gluon plasma (QGP) probe. We propose the appearance of a local minimum at midrapidity for the charge transfer fluctuation as a signal for a QGP. Within a two-component neutral cluster model, we demonstrate that the charge transfer fluctuation can detect the presence of a QGP as well as the size of the QGP in the rapidity space. We also show that the forward-backward correlation of multiplicity can be a similarly good measure of the presence of a QGP. Further, we show that the previously proposed net charge fluctuation is sensitive to the existence of the second phase only if the QGP phase occupies a large portion of the available rapidity space.

DOI: 10.1103/PhysRevC.72.034904 PACS number(s): 25.75.−q, 12.38.Mh, 24.60.−k

I. INTRODUCTION

Active research in relativistic heavy-ion collisions has given us much information about the hot matter produced in such collisions. Much attention has been directed to the question of whether a deconfined quark-gluon plasma (QGP) phase has been formed. The experimental studies do suggest that strongly interacting dense matter was formed during the early stage of reaction, and the energy density of such matter is very high (see [1–5] and references therein). Most theoretical models for such hot and dense matter explicitly invoke quark and gluon degrees of freedom in the elementary processes [6–19]. One way to detect the presence of a QGP is then to measure the changes in the fluctuations and correlations that could originate from the new phase of matter.

In this work, we propose charge transfer fluctuations as a signal of the presence of a QGP as well as a measure of the (longitudinal) size of the QGP. Charge transfer fluctuation for elementary collisions was originally proposed by Quigg and Thomas [20], who considered a flat charged particle distribution $dN_{\rm ch}/dy$. This idea was later extended to smooth distributions by Chao and Quigg [21].

The central result of Refs. [20,21] is the relationship between the single-particle distribution function $dN_{\rm ch}/dy$ and the charge transfer fluctuation:

$$D_u(y) = \kappa \frac{dN_{\rm ch}}{dy}, \tag{1}$$

where κ is a constant and

$$D_u(y) \equiv \langle u(y)^2 \rangle - \langle u(y) \rangle^2 \tag{2}$$

is the charge transfer fluctuation. The charge transfer $u(y)$ is defined by the forward-backward charge difference:

$$u(y) = [Q_F(y) - Q_B(y)]/2, \tag{3}$$

where $Q_F(y)$ is the net charge in the rapidity region forward of y and $Q_B(y)$ is the net charge in the rapidity region backward of y. The fluctuation $D_u(y)$ is then a measure of the correlation between the charges in the forward and the backward regions separated by y.

The importance of the relationship (1) lies in the fact that κ is directly proportional to the *local* unlike-sign charge correlation length. Heuristically, this can be explained in the following way. Suppose all final particles originate from neutral clusters and each cluster produces one positively charged particle and one negatively charged particle. Then the only way $u(y)$ can deviate from zero is when one charged particle from a cluster ends up in the forward region while the other ends up in the backward region, as illustrated in Fig. 1. For each one of these split pairs, the charge transfer $u(y)$ undergoes a 1-D random walk with a step size 1. Therefore, the charge transfer fluctuation $D_u(y)$ should be proportional to the number of split pairs, or equivalently the number of random steps taken.

If λ is the typical rapidity difference between the two decay particles from a single cluster, then only the clusters within the rapidity interval $(y - \lambda/2, y + \lambda/2)$ can contribute to $D_u(y)$, as illustrated in Fig. 1. The number of such clusters is then $\lambda dN_{\rm clstr}/dy$, where $dN_{\rm clstr}/dy$ is the density of the clusters at y. Since the final particle spectrum $dN_{\rm ch}/dy$ should be proportional to $dN_{\rm clstr}/dy$, we have Eq. (1) with $\kappa \propto \lambda$. Hence the ratio $\kappa = D_u(y)/(dN_{\rm ch}/dy)$ is a measure of the *local* environment near y: If λ is a function of y, then $\kappa(y)$ should also change accordingly.

The fact that κ is constant in elementary collisions indicates that in such collisions the correlation length is constant throughout the entire rapidity range (see [21,22] and references therein). However, if a QGP is produced in the central region of the relativistic heavy-ion collisions, we can expect the local charge correlation length $\lambda(y)$ to increase as y moves away from central rapidity. This is because the charge correlation length in a QGP is expected to be much smaller than that in a

*Electronic address: shil@physics.mcgill.ca
†Electronic address: jeon@physics.mcgill.ca

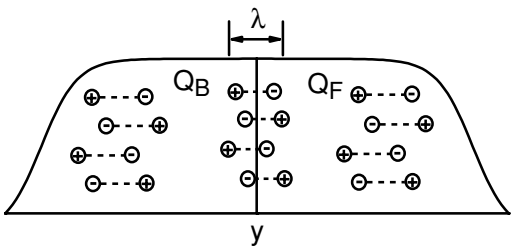

FIG. 1. A schematic illustration of the charge transfer fluctuations in rapidity space. Only pairs within $\lambda/2$ of y can contribute to the charge transfer fluctuation $D_u(y)$. Here λ is the rapidity correlation length, or the rapidity distance of the decay particles from a single cluster. If λ is a function of y, then $D_u(y)$ also changes with y.

hadronic phase [23,24]. In this case, the ratio

$$\kappa(y) = \frac{D_u(y)}{dN_{\rm ch}/dy} \tag{4}$$

will vary from a smaller value to a larger value as one goes away from the central region toward the forward region.

There have been many studies of the fluctuations and correlations in heavy-ion collisions [23,25–42]. Most of these studies concentrate on *global* information and do not address possible spatial inhomogeneity of the created matter in relativistic heavy-ion collisions. For instance, if the QGP phase is confined to a small rapidity region, the net charge fluctuation measures proposed in Refs. [30,31] may not be very sensitive to the presence of a QGP. Hence negative results from experiments [32,34,35] do not necessarily exclude the formation of a QGP.

Our expectation that the central rapidity region in heavy-ion collisions is mostly QGP originates from Bjorken's seminal work [43]. In that paper it was assumed that the expanding QGP evolves in a boost-invariant manner. Such an assumption naturally leads to the expectation that the central plateau in the rapidity spectrum is a manifestation of a boost-invariant QGP. However, recent RHIC results cast some doubts on the boost-invariant scenario in the central rapidity region: Although the charged particle distributions as a function of pseudorapidity shows a central plateau [44,45], the recent *rapidity* spectrum of charged particles from the BRAHMS group is consistent with a Gaussian following the Landau picture [46], although a plateau within $-1 < y < 1$ cannot be ruled out [47]. The elliptic flow spectrum from the PHOBOS group [48] shows no discernible plateau at all as a function of pseudorapidity. Thus, a simple boost-invariant scenario in a large range of rapidity space as originally envisioned by Bjorken [43] may not be valid. If the QGP phase is produced in relativistic heavy-ion collisions, a pure phase may very well be confined to a fairly limited rapidity range. It is, therefore, important to have an observable that is sensitive to the *local* presence of a QGP. The charge transfer fluctuation is such a local measure of a phase change.

Of course, as emphasized in Ref. [49], a particular type of fluctuation is just one particular aspect of the underlying correlations. The usefulness of each type of fluctuation then depends on the sensitivity of the chosen fluctuation to an interesting aspect of the correlation. For charge transfer fluctuations, that aspect is the size of the local charge correlation length. Hence if the QGP phase is spatially confined to a narrow region around midrapidity, the charge transfer fluctuations can signal its presence and also can yield information about the size.

In this study, we propose the appearance of a clear minimum at midrapidity for the ratio $\kappa(y)$ as a signal for the existence of two different phases. The slope and the size of the dip around midrapidity can then reveal the size of the new phase (presumably a QGP). These features should disappear as the energy is lowered or the collisions become more peripheral where a QGP is not expected to form.

In the following, we use a single-component neutral-cluster model and a two-component neutral-cluster model to study the purely hadronic case and the mixed-phase case. However, the fact that the charge transfer fluctuation is a useful measure of the *local* correlation length is independent of our particular choice of models. Hence we expect that the general conclusions drawn in this study should be valid even within more sophisticated models as well as in real experimental situations. A case study using several cascade models is under way.

We note here that most of the discussions in this study are in terms of the rapidity y. However, the validity of our results does not depend very much on whether we use rapidity y or the pseudorapidity η. We also note that the argument given here applies with very little change to any conserved charges such as the baryon number.

The rest of this paper is organized as follows: In the next section, we consider the basic phenomenology of the charge transfer fluctuations. In Sec. III, we consider the net charge fluctuations and the charge transfer fluctuations in a single-component model. In Sec. IV, we present our main results for a two-component model. It is proposed that the presence of a rising segment of the charge transfer fluctuation as a function of rapidity can be used as a QGP signal. We also show that the charge transfer fluctuation can reveal the size of the QGP. A summary is given in Sec. V.

II. CHARGE TRANSFER FLUCTUATIONS

The charge transfer is defined in Eq. (3). The charge transfer fluctuation is defined in Eq. (2). Originally Quigg and Thomas [20], considering a flat $dN_{\rm ch}/dy$, argued that if all hadrons originated from neutral clusters, then the following relation should hold:

$$D_u(0) = \frac{4\lambda}{3}\frac{N_{\rm ch}}{Y_{\rm max}}, \tag{5}$$

where λ is the rapidity correlation length of unlike-sign $(+-)$ pairs originating from a single neutral cluster, $N_{\rm ch}$ is the total multiplicity of the produced charged particles, and $Y_{\rm max}/2$ is the beam rapidity in the c.m. frame.

Later, this was extended by Chao and Quigg to smooth charged particle distributions [21] to yield Eq. (1), $D_u(y) = \kappa dN_{\rm ch}/dy$, with $\kappa \propto \lambda$. The experimental results on pp and $K^- p$ collisions show that this relationship is remarkably good with κ ranging from 0.62 to 0.85 (see [21,22] and references therein). We have replotted 205-GeV pp collision results from Ref. [22] in Fig. 2. Here the proportionality constant κ is

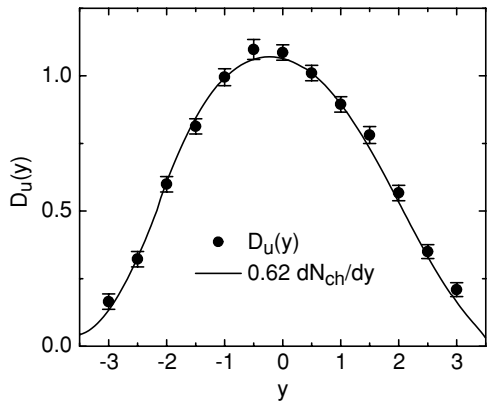

FIG. 2. The charge transfer fluctuation results from *pp* collisions at a beam energy of 205 GeV is shown as a function of rapidity. The line is the charge yield profile measured in the same reaction scaled by a factor of 0.62. This is a replot of the results reported in [22].

approximately 0.62. As we shall see later in this section, the proportionality of the charge transfer fluctuation to the charged particle spectrum is a strong argument for correlated charge pairs instead of uncorrelated charged particles.

The charge correlation length λ measures the rapidity correlations between unlike-sign charges. (This quantity also plays a central role in two of the proposed QGP signals, namely the net charge fluctuations and the balance function.) To illustrate the relationship between the proportionality constant κ and the unlike-sign charge correlation length λ in Eq. (1), we consider a simple "ρ" gas model (see e.g., [50]).

In this model, each $\rho^{\pm}$ is assumed to decay to a $\pi^0\pi^{\pm}$ pair and each ρ^0 is assumed to decay to a $\pi^+\pi^-$ pair. This is similar to the ρ and ω models used for *pp* collisions [21,51]. One should not, of course, regard these ρ's as physical ρ mesons. These are just convenient names for charged and neutral clusters. In particular, they are not isospin triplets.

Consider a set of events where M_0 number of ρ^0's and M_+ and M_- number of ρ^+'s and ρ^-'s are produced. The full joint probability for the rapidity of the charged pions for this set is given by

$$\rho(\{y_a\}) = \prod_{i=1}^{M_+} g(y_i) \prod_{j=1}^{M_-} g(y_j) \prod_{k=1}^{M_0} f_0(y_k^+, y_k^-), \tag{6}$$

where $f_0(y^+, y^-)$ is the probability for the two decay products of a neutral cluster to have the rapidities y^+ and y^- and $g(y)$ is the single-particle distribution function for the charged particles originating from the charged ρ's. Averaging over the distributions of M_0, M_+, and M_- with the condition $Q = M_+ - M_- =$ constant, we can easily show that

$$D_u(y) = 2\langle M_0\rangle \int_{-\infty}^{y} dy' \int_{y}^{\infty} dy'' f_0(y', y'') + \langle M_{\rm ch}\rangle \int_{-\infty}^{y} dy' g(y') \int_{y}^{\infty} dy'' g(y''), \tag{7}$$

where $M_{\rm ch} = M_+ + M_-$. In arriving at this result, we neglected a contribution that is on the order of $\langle u(y)\rangle^2/N_{\rm ch} \sim Q^2/N_{\rm ch}$, where $N_{\rm ch} = 2\langle M_0\rangle + \langle M_{\rm ch}\rangle$. This should be small compared to the terms in Eq. (7) when $Q \ll N_{\rm ch}$. See Appendix B for details.

The single-particle rapidity distribution is given by

$$\frac{dN_{\rm ch}}{dy} = 2\langle M_0\rangle h(y) + \langle M_{\rm ch}\rangle g(y), \tag{8}$$

where $h(y) = \int_{-\infty}^{\infty} dy' f_0(y', y)$.

The Thomas-Chao-Quigg relationship, $D_u(y) = \kappa dN_{\rm ch}/dy$, can be solved explicitly in two extreme cases when either $M_0 = 0$ or $M_{\rm ch} = 0$. When $M_0 = 0$, we have

$$\int_{-\infty}^{y} dy' g(y') \int_{y}^{\infty} dy'' g(y'') = \kappa g(y) \tag{9}$$

and the solution is given by

$$g(y) = \frac{1}{4\kappa} \mathrm{sech}^2\left(\frac{y}{2\kappa}\right), \tag{10}$$

which can be easily verified using $\mathrm{sech}^2 x = d\tanh x/dx = 1 - \tanh^2 x$. With $\kappa = O(1)$, this form alone (basically the modified Pöschl-Teller potential) is much too sharp to describe a realistic $dN_{\rm ch}/dy$. Furthermore, it has no room for energy dependence once κ is fixed. This contrasts with the $dN_{\rm ch}/dy$ spectrum in elementary collisions, which shows no prominent central peak of a fixed width. Hence the $M_0 = 0$ scenario can be excluded.

In the $M_{\rm ch} = 0$ limit, the Thomas-Chao-Quigg relationship is

$$\int_{-\infty}^{y} dy' \int_{y}^{\infty} dy'' f_0(y', y'') = \kappa \int_{-\infty}^{\infty} dy' f_0(y', y), \tag{11}$$

To solve for $f_0(y, y')$, we make an ansatz

$$f_0(y, y') = R(y_{\rm rel}) F(Y), \tag{12}$$

where $y_{\rm rel} = y - y'$ and $Y = (y + y')/2$. The normalization conditions for R and F are $\int_{-\infty}^{\infty} dy R(y) = \int_{-\infty}^{\infty} dy F(y) = 1$. Equation (11) can then be solved by making a change of variables to $y_{\rm rel}$ and Y. The solution is

$$f_0(y, y') = \frac{1}{4\kappa} \exp\left(-\frac{|y - y'|}{2\kappa}\right) F\left(\frac{y + y'}{2}\right), \tag{13}$$

where the only restriction on F is that the integrals in Eq. (11) converge and it reproduces the experimental $dN_{\rm ch}/dy$. For details, see Appendix C. This form of correlation function is very reasonable as it is nothing but the distribution function of the decay products of a cluster whose rapidity is distributed according to $F(Y)$.

For small enough κ, we should have

$$F(y) \approx \frac{1}{N_{\rm ch}} \frac{dN_{\rm ch}}{dy}, \tag{14}$$

where $N_{\rm ch} = 2\langle M_0\rangle$ is the total charge multiplicity. In this solution, it is clear that κ is directly related to the correlation length λ in the relative rapidity space of the pair $y - y'$ because

$$\lambda = 2\kappa. \tag{15}$$

By taking the correlation $\kappa \sim 1$, it is easy to see that the charged particle spectrum will be a smooth distribution with typical variation in rapidity of $2\kappa \sim 2$. This is in good agreement with the *pp* collision results in Fig. 2. Further, the absence

of a narrow peak in the central region also excludes any significant contribution from the uncorrelated charged particles.

If we have a finite observational window $(-y_o, y_o)$, the charge transfer fluctuations are given by

$$\bar{D}_u(y) = \frac{\langle M_0 \rangle}{2}\left[\int_{-y_o}^{y_o} dy' \int_{-\infty}^{-y_o} dy'' f_0(y', y'') + \int_{-y_o}^{y_o} dy' \int_{y_o}^{\infty} dy'' f_0(y', y'') + 4\int_{-y_o}^{y} dy' \int_{y}^{y_o} dy'' f_0(y', y'')\right] \quad (16)$$

where the bar in $\bar{D}_u$ indicates that this quantity is measured in a limited window. With a moderate y_o, the Thomas-Chao-Quigg relationship [Eq. (1)] no longer holds even if the unrestricted charge transfer fluctuation satisfies it. However, $\bar{D}_u(y)$ is still sensitive to the charge correlation length. To have an idea how $\bar{D}_u(y)$ behaves, we can use a flat $F(Y)$ following Thomas and Quigg. If κ is much smaller than the size of the total rapidity interval $Y_{\max}$ and y_o is not too close to $Y_{\max}/2$, we get

$$\frac{\bar{D}_u(y)}{\langle N_{\rm ch} \rangle} = \frac{\kappa}{2y_o}\left[\frac{3}{2} + \frac{1}{2}e^{-y_o/\kappa} - 2e^{-y_o/2\kappa}\cosh\left(\frac{y}{2\kappa}\right)\right]. \quad (17)$$

If we have a large y_o/κ, this becomes constant and we retrieve the original Thomas-Quigg relationship Eq. (5). With a finite y_o, this is a monotonically decreasing function of $y > 0$ with the maximum at $y = 0$.

The pseudorapidity distribution measured by RHIC experiments does show a plateau within $-2 < \eta < 2$ and the rapidity distribution shows a similar plateau within $-1 < y < 1$. Hence, if the correlation length (κ) remains constant throughout the plateau, one would expect that $\bar{D}_u(y)$ measured within the plateau should also have a maximum at $y = 0$. However, if one observes that $\bar{D}_u(y)$ has a *minimum* at $y = 0$, then it is a signal that quite a different system (a QGP) is created near the central rapidity with a much smaller rapidity correlation length than the rest of the system.

To examine the relationship between the charge transfer fluctuations and the charge correlation length, we must make sure that other effects such as the impact parameter fluctuations and the hadronic correlations do not mimic the effect we seek. To study the non-QGP effects, we have analyzed 50, 000 HIJING events [52]. The results are shown in Fig. 3. Each point in the figure represents a 5% bin in the centrality measured by the number of charged particles within $-1 < y < 1$. It is quite obvious from this figure that the charge transfer fluctuations do not vary with centrality. It is also obvious that $\bar{D}_u(y)$ in this case is a decreasing function of y.

It is interesting to compare Eq. (17) with the results from HIJING. For this, we used the top 15% central results in Fig. 3 and fitted them with Eq. (17). The best fit gives $\kappa = 0.72$ though the results from Eq. (17) are slightly flatter than the HIJING results. This discrepancy in shape is not unexpected because the HIJING $dN_{\rm ch}/dy$ is not well approximated by a flat $F(Y)$. The full pseudorapidity space analysis of 50, 000 HIJING minimum-bias events are shown in Fig. 4 for three different centralities. The Thomas-Chao-Quigg relationship works quite well within this model for all centrality classes. In the rapidity region of $y = 0$–3, the value of κ is in the range of 0.63–0.68. This is consistent with the experimental *pp* result.

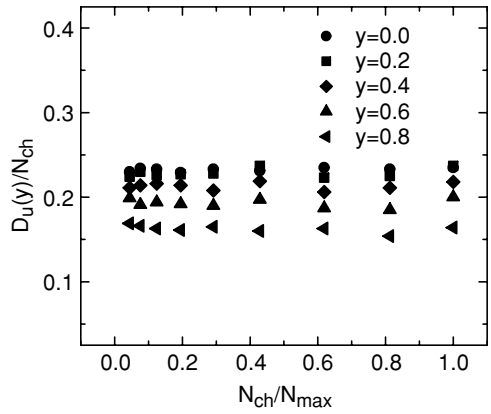

FIG. 3. The ratio of the charge transfer fluctuations to the number of charged particles, $\bar{D}_u(y)/N_{\rm ch}$, shown as a function of centrality $N_{\rm ch}/N_{\max}$. The observation window is fixed at $(-1.0, 1.0)$. These results are from a HIJING calculation for $\sqrt{s} = 200$ GeV Au-Au collisions. Parameters for the HIJING calculations are $dE/dx = 2$ GeV/fm and $p_{\rm minijet} = 2$ GeV with the shadow and the quench flags on. Each of the two most central bins has 5% of the events; all other bins contain 10%. A total of 50, 000 HIJING events are analyzed.

In the next two sections, we test our idea against two scenarios for heavy-ion collisions. In the first scenario, the created system consists of a single species of neutral clusters, which may be taken as hadronic clusters. In the second scenario, the created system contains a second component with a much smaller correlation length.

III. SINGLE-COMPONENT MODEL

In this section, we consider the charge transfer fluctuations in a system that consists of only a single species of neutral clusters (presumably hadronic matter).

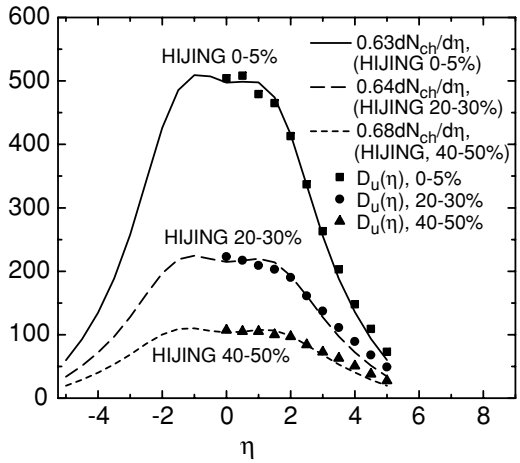

FIG. 4. The results of analyzing simulated Au-Au events using HIJING. The lines are scaled pseudorapidity spectra for centrality classes 0–5%, 20–30%, and 40–50% and the symbols are charge transfer fluctuations for each class.

The Thomas-Chao-Quigg relationship was used to justify the use of the neutral cluster model in *pp* collisions in the last section. For heavy-ion collisions, as far as we know there has been no experimental investigation in this area. For this study, we take the HIJING simulation results shown in Fig. 4 as an indication that the single-component neutral-cluster model is also a good *hadronic* model of *AA* collisions and explore the consequences. A case study with a few hadronic event generators is under way and will be reported elsewhere.

With only a single species of clusters, the joint probability to have an event with particle rapidities ($\{y_a\}$) is simply

$$\rho(\{y_a\}) = \prod_{k=1}^{M_0} f_0(y_k^+, y_k^-). \tag{18}$$

All observables in this model depend only on the pair distribution function $f_0(y^+, y^-)$. Hereafter, we will drop the subscript 0 from f_0 for brevity. This is pertinent to heavy-ion collisions at RHIC where the net charge is almost zero in the central region. For completeness, we have also listed the formulas for unpaired net charges in Appendix A. Further as discussed in Appendix B, the contribution of the nonzero net charges to the charge transfer fluctuations is negligible as long as $Q \ll N_{\rm ch}$.

Because of our assumption that the decay products are identical except for the electrical charges, the two-point function has the following symmetries:

$$f(y^+, y^-) = f(y^-, y^+), \tag{19a}$$

$$f(y^+, y^-) = f(-y^+, -y^-). \tag{19b}$$

We will use these symmetry properties to simplify the equations for the charge transfer fluctuations and the net charge fluctuations.

Guided by our discussion of the Thomas-Chao-Quigg relationship, we use a separable form of pair distribution function $f(y^+, y^-) = F(Y)R(y_{\rm rel})$, where $Y = (y^+ + y^-)/2$ and $y_{\rm rel} = y^+ - y^-$ as in Eqs. (12) and (13). The function $F(Y)$ is the rapidity distribution of the clusters and the function $R(y_{\rm rel})$ is the relative rapidity distribution of the produced pair. For the shape of $F(Y)$, we use a Woods-Saxon form and a Gaussian form here but more sophisticated forms are certainly possible. For $R(y_{\rm rel})$, the following two physically motivated forms were used in our study:

$$R(r) = \frac{1}{\gamma\sqrt{2\pi}} \exp(-r^2/2\gamma^2), \tag{20a}$$

$$R(r) = \frac{1}{2\gamma} \exp(-|r|/\gamma). \tag{20b}$$

The function in Eq. (20b) is the same as Eq. (13) with $\gamma = 2\kappa$.

The combination of $F(Y)$ and $R(r)$ are not arbitrary. Once we fix the charge correlation length γ for a particular $R(r)$, then the parameters for $F(Y)$ are complete determined by the best fit to the experimental charged particle distributions [44,53]. To test the sensitivity to the different forms of the correlation function, we use the following four parameter sets in this section: Parameter set 1 uses a Woods-Saxon form of $F(Y)$ and a Gaussian $R(y_{\rm rel})$. Set 2 uses a Woods-Saxon $F(Y)$ but $R(y_{\rm rel})$ has an exponential from. Parameter set 3 uses a Gaussian $F(Y)$ and also a Gaussian $R(y_{\rm rel})$. Set 4 uses a Gaussian $F(Y)$ but $R(y_{\rm rel})$ has an exponential form. These parameter sets will be used for the net charge fluctuation analysis and the charge transfer fluctuation analysis.

A. Net charge fluctuation

The STAR Collaboration at RHIC has published its measurement of net charge fluctuations [35] and concluded that its result is consistent with hadronic gas expectations. In this section, we use this data to fix the correlation length γ. Since our previous fit to the HIJING simulations gave $\gamma \sim 1.3$–1.4, we will look for the correlation length within the range of $1 < \gamma < 2$.

Within the observation window $-y_{\rm o} < y < y_{\rm o}$, the net charge and the charge transfer are given by

$$\begin{aligned} u(y) &= [Q_F(y) - Q_B(y)]/2, \\ Q(y_{\rm o}) &= [Q_F(y) + Q_B(y)], \end{aligned} \tag{21}$$

where now $Q_F(y)$ and $Q_B(y)$ are measured within the observational window. Notice that $Q(y_{\rm o})$ is actually independent of y. In the limit $y = y_{\rm o}$, we have $u = Q/2$.

In terms of the charge pair distribution function, the net charge fluctuation is given by

$$\begin{aligned} \delta Q^2(y_{\rm o}) &= \langle Q(y_{\rm o})^2\rangle - \langle Q(y_{\rm o})\rangle^2 \\ &= 4\langle M_0\rangle \int_{-\infty}^{-y_{\rm o}} dy^- \int_{-y_{\rm o}}^{y_{\rm o}} dy^+ f(y^+, y^-). \end{aligned} \tag{22}$$

In deriving Eq. (22), we have made full use of the symmetry properties of the pair distribution function, Eqs. (19). Since the two-particle distribution function $f(y^+, y^-)$ is peaked at $|y^+ - y^-| = 0$, the net charge fluctuations in Eq. (22) measure the local correlations at around the edge of the observation window $y \sim \pm y_{\rm o}$. One can also see, that, as $y_{\rm o} \to \infty$, the net charge fluctuation vanishes as it must.

The total number of charged particles in the given rapidity window $(-y_{\rm o}, y_{\rm o})$ is

$$N_{\rm ch}(y_{\rm o}) = 2\langle M_0\rangle \int_{-y_{\rm o}}^{y_{\rm o}} dy^- \int_{-\infty}^{\infty} dy^+ f(y^+, y^-). \tag{23}$$

The ratio of the net charge fluctuations to the total number of charges in the rapidity window $(-0.5, 0.5)$ was measured in the RHIC experiments, and the value for central collisions is around $\delta Q^2/N_{\rm ch} = 0.8$–$0.9$ after correcting for the global charge conservation effect [34,35]. The correction is made through a factor of $1/(1-p)$, where p is the fraction of the charged particles included in the observation compared to the total number of charged particles produced. From this value, we can find the correlation length for charged pairs. The exact value depends slightly on the assumption on the shape of the pair correlation function $R(r)$ in relative rapidity space and the charge center distribution $F(Y)$.

In Fig. 5, we have plotted the ratio of the net charge fluctuations to the total number of charges, $\delta Q^2(y_{\rm o})/N_{\rm ch}(y_{\rm o})$, as a function of the pair correlation length γ. We only show here the charge fluctuation results from parameter set 2,

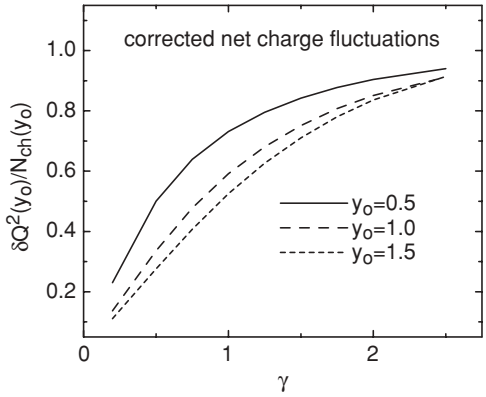

FIG. 5. The charge-conservation-corrected ratio of the net charge fluctuations to the total number of charged particles, $\delta Q^2(y_o)/N_{ch}(y_o)$, shown as a function of the charge correlation length γ. We show the ratio at three different rapidity observation windows, $|y| < y_o$, where $y_o = 0.5$, 1.0, and 1.5 for the three lines, respectively. The parameters for the charge pair center distribution function $F(y)$ are adjusted to fit the charged particle distribution data measured by the PHOBOS group at $\sqrt{s} = 130$ GeV.

where the charge center distribution $F(Y)$ is of Woods-Saxon form and the relative rapidity distribution between the pair $R(r)$ is an exponential decay. The different assumed forms of the pair distribution function $f = F(y)R(r)$ have little effect on the net charge fluctuations and are not show here for clarity. From this figure, one can conclude that the net charge fluctuations $\delta Q^2(y_o)$ are strongly correlated with the charge correlation length γ in this single-component case.

RHIC experiments can measure the net charge fluctuations as a function of the observational window size y_o. We have plotted the corrected net charge fluctuations as a function y_o in Fig. 6. As can be seen in this figure, the net charge fluctuations always decrease when the observation window is enlarged. This is because the total number of charged particles included in the observation window is increasing faster than the net charge fluctuations. The slope, however, is related to the charge correlation length.

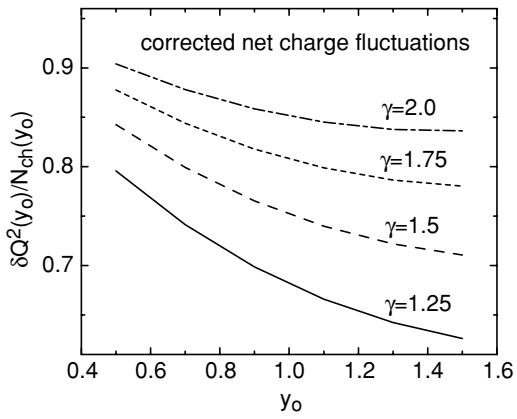

FIG. 6. The corrected net charge fluctuation ratio $\delta Q^2(y_o)/N_{ch}(y_o)$ shown as a function of the observation window size y_o for different values of charge correlation lengths $\gamma = 1.25$, 1.5, 1.75, and 2.0, respectively. The net charge fluctuations are decreasing functions of the observation window.

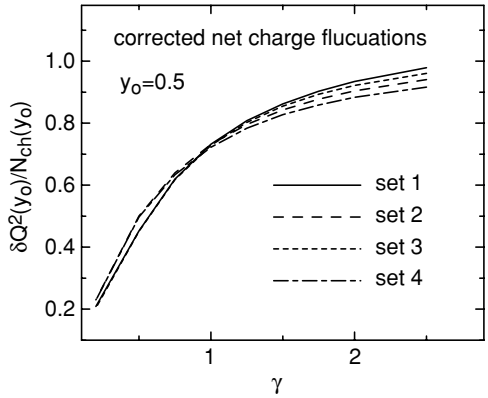

FIG. 7. The charge-conservation-corrected ratio of the net charge fluctuations to the total number of charged particles plotted as a function of the charge correlation length γ. Set 1 refers to a Woods-Saxon form for the charge pair center distribution $F(y)$ and to a Gaussian form for the relative rapidity distribution between the pair $R(r)$. Set 2 refers to a Woods-Saxon form for $F(y)$ and to an exponential decay form for $R(r)$. Sets 3 and 4 are for a Gaussian form of $F(y)$ with a Gaussian or exponential decay form of $R(r)$, respectively. These results should be compared with data reported for $\sqrt{s} = 130$ GeV Au-Au collisions at RHIC. Here the observation window is $(-0.5, 0.5)$ in rapidity.

Using the corrected net-charge-fluctuation ratio data from STAR [35], we deduce that the charge correlation length is

$$\gamma \approx 1.5. \tag{24}$$

This deduced value is largely independent of the shape of the charge pair correlation function $R(r)$ or the pair center distribution function $F(Y)$, as shown in Fig. 7. Notice that the inferred charge correlation length is consistent with the HIJING results, where $\kappa = \gamma/2 \approx 0.7$ in the previous simple estimate within the rapidity window $(-1, 1)$.

B. Charge transfer fluctuations

We now apply our model to the charge transfer fluctuations using the same parameter sets for the pair distribution function $f(y^+, y^-)$ as we have used in the last section.

First, we need to express the charge transfer fluctuations in terms of the pair distribution function $f(y^+, y^-)$. With Eq. (23), we can simplify Eq. (16) to

$$\begin{aligned}\bar{D}_u(y) &= \frac{\delta Q^2(y_o)}{4} - \langle \delta Q_F(y)\, \delta Q_B(y) \rangle \\ &= \frac{\delta Q^2(y_o)}{4} + 2\langle M_0 \rangle \int_{-y_o}^{y} dy^- \int_{y}^{y_o} dy^+ f(y^+, y^-),\end{aligned} \tag{25}$$

where we have defined $\delta X \equiv X - \langle X \rangle$. Written this way, it is clear that the charge transfer fluctuations depend on the charge correlations both at the edges of the observation window $y \sim \pm y_o$ and at the forward-backward rapidity cut y. From this expression, one also sees that the lower limit of charge transfer fluctuations is $\{\bar{D}_u(y)\}_{\min} = \delta Q^2(y_o)/4$.

In Fig. 8, we have plotted the ratio of the charge transfer fluctuation $\bar{D}_u(y)$ to the charged particle yield dN_{ch}/dy as a function of pair correlation length γ. Because the observed

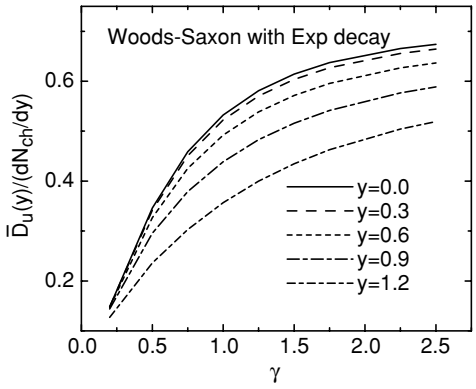

FIG. 8. The ratio of the charge transfer fluctuations $\bar{D}_u(y)$ to the charged particle yield $dN_{\rm ch}/dy$ in the observation window $(-1.5, 1.5)$ plotted as a function of the charged particle correlation length γ. The different lines represent the results for different forward-backward rapidity cuts, $y = 0.0, 0.3, 0.6, 0.9$, and 1.2, respectively. We only show results from parameter set 2; other parameter sets yield qualitatively similar results. These results are for the one-component model.

rapidity spectrum is nearly flat around midrapidity, dividing by $N_{\rm ch}$ or $dN_{\rm ch}/dy$ only affects the overall scale. The value of the ratio strongly depends on the correlation length γ. Also, the ratio decreases as the forward-backward separation y increases at a fixed γ. As mentioned before [cf. Eq. (17)], this decrease is due to the limited observation window and has nothing to do with the changing correlation length. This can also be shown in the following way. If $dN_{\rm ch}/dy$ does not vary significantly within the observational window, then $F(Y)$ does not vary significantly within the observational window. In that case,

$$\frac{1}{\langle M_0\rangle}\frac{\partial \bar{D}(y)}{\partial y} \approx -F(0)\int_{y_o-y}^{y_o+y} dr\, R(r) < 0 \qquad (26)$$

for $y > 0$. Therefore, if $dN_{\rm ch}/dy$ is flat *and* the system is composed of only one species of neutral clusters, $\bar{D}_u(y)$ must be a decreasing function of $y > 0$. Conversely, if $\bar{D}_u(y)$ is an *increasing* function of $y > 0$ while $dN_{\rm ch}/dy$ remains flat, it signals the existence of a new component. We turn to this possibility in the next section.

IV. TWO-COMPONENT MODEL

In a two-component model, the full joint probability for the rapidities is given by

$$\rho(\{y_i\}) = \prod_{j=1}^{M_1} f_1(y_j^+, y_j^-)\prod_{k=1}^{M_2} f_2(y_k^+, y_k^-), \qquad (27)$$

where f_1 and f_2 have different correlations lengths $\gamma_1 > \gamma_2$. The pair distribution functions are again taken as the separable form: $f_i(y^+, y^-) = F_i(Y)R_i(r)$, where $Y = (y^+ + y^-)/2$ and $r = y^+ - y^-$. Since the fluctuations add in quadrature, the net charge fluctuations and the charge transfer fluctuations are just the sum of contributions from the two components, f_1 and f_2, respectively.

Physically, the two-component model is motivated by the fact that the hot and dense matter produced in the relativistic heavy-ion reaction is not necessarily homogeneous in rapidity space as explained before. If the deconfined QGP phase did exist during the early stage of heavy-ion reaction, it is highly possible that the QGP phase coexisted with the hadron gas phase. A simple situation would be a phase separation between the QGP phase and the hadron gas phase. This could produce signals that are specific to a phase coexistence scenario. In the case of the charge transfer fluctuations, a QGP and hadron gas phase separation could be measured and mapped into the charge correlations in the relative rapidity space between the pair of particles. In the following, we will refer to the short correlation part as a QGP and the long correlation part as a hadron gas (HG).

In our simple two-component model, we assume the two components have different correlation lengths and the $R(r)$ functions are either taken as an exponential form or a Gaussian form, with the corresponding correlation lengths satisfying $\gamma_1 > \gamma_2$. Here $\gamma_1 = \gamma_{\rm HG}$ is the rapidity correlation length of the hadronic part (labeled 1) and $\gamma_2 = \gamma_{\rm QGP}$ is that of the QGP part (labeled 2). We let the cluster distribution functions for the two components be

$$\langle M_1\rangle F_1(y) = \frac{c_1}{1+\exp[(|y|-\sigma_0)/a_0]} - c_2 g_1(y), \qquad (28a)$$

$$\langle M_2\rangle F_2(y) = c_2 g_2(y), \qquad (28b)$$

where c_1 is a normalization factor and c_2 is the strength of the QGP phase. To be physically consistent, the value of c_2 is adjusted so that the function F_1 is always positive. We then demand that $\int R_1 g_1 = \int R_2 g_2$ so that $dN_{\rm ch}/dy$ is independent of the choices of g_1 and g_2. The parameters σ_0 and a_0 are chosen to fit the experimental data.

For a Gaussian $R_i(r)$, it is convenient to also take the functional forms of $g_1(y)$ and $g_2(y)$ to be Gaussian. To satisfy $\int R_1 g_1 = \int R_2 g_2$, the widths of these Gaussians should be related as follows: $\xi^2 = \gamma_1^2/4 + \sigma_1^2 = \gamma_2^2/4 + \sigma_2^2$, where σ_i is the width of $g_i(y)$ and ξ is the width of the QGP part of $dN_{\rm ch}/dy$. For an exponential $R_i(r)$, determining the forms of g_1 and g_2 is a little more complicated than for the Gaussian case. However, since this form of the correlation function satisfies the Thomas-Chao-Quigg relationship, we will use mainly the exponential form hereafter. As in the one-component model, both the net charge fluctuation and the charge transfer fluctuation results are not very sensitive to the particular choice of functional form of the two-particle distribution function.

With the exponential $R_i(r)$, the charge center distribution functions $g_1(y)$ and $g_2(y)$ can no longer both be Gaussian. It is convenient to select $g_1(y)$ (the hadronic part) to have a Gaussian form. By using the fact that the function $R_i(r)$ is in fact a Green function of the differential operator $(d/dr)^2 - 1/\gamma_i^2$, the function $g_2(y)$ (the QGP part) can be obtained as

$$g_2(y) = \left(\frac{\gamma_2}{\gamma_1}\right)^2 g_1(y) + \left[1 - \left(\frac{\gamma_2}{\gamma_1}\right)^2\right]\rho(y), \qquad (29)$$

where $\rho(y) = \int R_1 g_1 = \int R_2 g_2$ is

$$\rho(y) = \int_{-\infty}^{\infty} dx\, g_1\left(\frac{x+y}{2}\right)\frac{1}{2\gamma_1}\exp\left(-\frac{|x-y|}{\gamma_1}\right). \qquad (30)$$

The function $\rho(y)$ is proportional to $dN_{\rm ch}/dy$ of the QGP part. The width ξ of the QGP part is determined by the width of $\rho(y)$.

In all, we have eight parameters here. We have c_1, σ_0, a_0, and c_2 explicitly appearing in Eq. (28). The parameter σ_1 is the width of the function g_1. The parameter ξ is the width of the function $\rho(y)$ and is connected with the parameter σ_1 through Eq. (30). We also have two charge correlation lengths γ_1 and γ_2 with the condition $\gamma_1 > \gamma_2$.

Among the eight parameters, five are fixed in the following way. Since we are only interested in the ratio $D_u(y)/(dN/dy)$, the value of parameter c_1 is irrelevant and we just fix it to be 1. The parameters a_0 and σ_0 are fixed by requiring that the resulting dN/dy shape describes results from RHIC experiments. The parameter c_2 is always chosen to be the maximum possible value for the condition $F_1(y) \geqslant 0$ given all other parameters. The parameter σ_1 is determined by the parameter ξ.

The three parameters we are going to vary in the following are then γ_1, γ_2, and ξ. An example of the total charged particle spectrum along with the respective hadron gas and QGP contributions is plotted in Fig. 9. There is a substantial presence of QGP around midrapidity, but it becomes less prominent for $|y| > \xi$.

A. Net charge fluctuation

As in the one-component model, we first consider the net charge fluctuations to further fix our parameters. When there are two distinct species of neutral clusters, the net charge fluctuation within the rapidity interval $(-y_{\rm o}, y_{\rm o})$ is given by

$$\delta Q^2(y_{\rm o}) = 4\langle M_1\rangle \int_{-\infty}^{-y_{\rm o}} dy^- \int_{-y_{\rm o}}^{y_{\rm o}} dy^+ f_1(y^+, y^-) + 4\langle M_2\rangle \int_{-\infty}^{-y_{\rm o}} dy^- \int_{-y_{\rm o}}^{y_{\rm o}} dy^+ f_2(y^+, y^-) \quad (31)$$

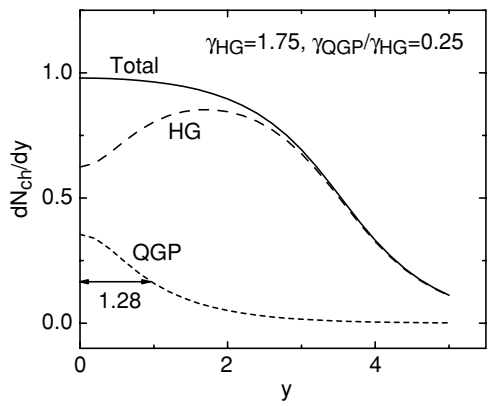

FIG. 9. The charge yields plotted as a function of rapidity in a two-component system. The full line represents the total charged particle yield profile; the dashed and dotted lines represent the contributions from the hadron gas and the QGP phases, respectively, in a typical two-component model we used. The QGP size is $\xi = 1.28$ in this case.

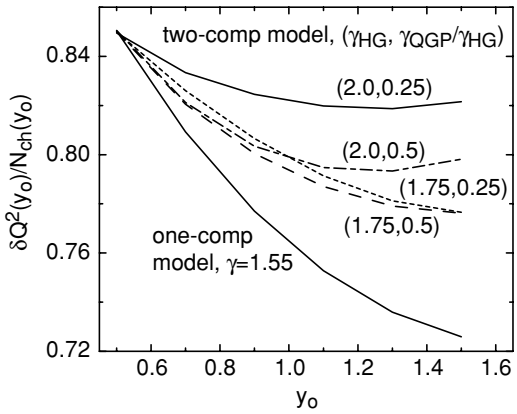

FIG. 10. The ratios of the corrected net charge fluctuations to the total number of charges, $\delta Q^2(y_{\rm o})/N_{\rm ch}(y_{\rm o})$, in the rapidity observation window $(-y_{\rm o}, y_{\rm o})$ plotted as a function of rapidity $y_{\rm o}$ for the one- and two-component models. The line for the one-component model is labeled by the charge correlation length $\gamma = 1.55$, and the lines for the two-component models are labeled by the pair of charge correlation lengths in the two components $(\gamma_{\rm HG}, \gamma_{\rm QGP}/\gamma_{\rm HG})$. The corrected net charge fluctuations are fixed at $\delta Q^2(0.5)/N_{\rm ch}(0.5) = 0.85$ for all lines.

and the total charged multiplicity is given by

$$N_{\rm ch}(y_{\rm o}) = 2\langle M_1\rangle \int_{-y_{\rm o}}^{y_{\rm o}} dy^- \int_{-\infty}^{\infty} dy^+ f_1(y^-, y^+) + 2\langle M_2\rangle \int_{-y_{\rm o}}^{y_{\rm o}} dy^- \int_{-\infty}^{\infty} dy^+ f_2(y^-, y^+). \quad (32)$$

The ratios $\delta Q^2(y_{\rm o})/N_{\rm ch}(y_{\rm o})$ corrected as before by a factor of $1/(1-p)$ are plotted as a function of the observation box size $y_{\rm o}$ in Fig. 10. The lowest solid line is for the one component model with charge correlation length $\gamma = 1.55$ as obtained in the last section. For the two-component model, four different choices with $\gamma_1 = \gamma_{\rm HG} = 1.75, 2.0$ and $\gamma_2/\gamma_1 = \gamma_{\rm QGP}/\gamma_{\rm HG} = 0.25, 0.5$ are shown. Since the corrected net charge fluctuations at $y_{\rm o} = 0.5$ is about 0.8–0.9 [34,35], the QGP width parameters ξ are chosen in such a way that all net charge fluctuations have $\delta Q^2(y_{\rm o})/N_{\rm ch}(y_{\rm o}) = 0.85$ at $y_{\rm o} = 0.5$. For instance, for the parameter set $\gamma_{\rm HG} = 1.75$ and $\gamma_{\rm QGP} = \gamma_{\rm HG}/4 = 0.44$, the width of the QGP part ξ turned out to be $\xi = 1.28$.

The net charge fluctuations as a function of rapidity is flatter in the two-component model than in the one-component model. This is because the two-component results interpolate between the one-component results with $\gamma = \gamma_{\rm QGP}$ and $\gamma = \gamma_{\rm HG}$. Since the behaviors of the net charge fluctuations for the one-component model and the two-component model are clearly distinct, one is tempted to argue that the flat $\delta Q^2(y_{\rm o})/N_{\rm ch}(y_{\rm o})$ itself is an indication of a second phase. (A similar idea was suggested in Ref. [54].) Unfortunately, a totally uncorrelated system also has a flat $\delta Q^2(y_{\rm o})/N_{\rm ch}(y_{\rm o})$ when corrected for the effect of total charge conservation.

In addition, the net charge fluctuation $\delta Q^2(y_{\rm o})/N_{\rm ch}(y_{\rm o})$ is constrained by the fact that, in the limit $y_{\rm o} \to 0$, we should get the Poisson limit $\delta Q^2(y_{\rm o})/N_{\rm ch}(y_{\rm o}) \to 1$. This puts a constraint on the sensitivity of net charge fluctuations to the QGP phase. In our two-component model, the QGP phase is located mostly

around midrapidity, and the presence of QGP is reduced at larger rapidities. Hence to observe the QGP, we need to have $y_o \sim 0$. But because of the limiting value at $y_o = 0$, the net charge fluctuations actually have a reduced sensitivity to the QGP phase. The charge transfer fluctuation, to which we now turn our attention, does not have these limitations.

B. Charge transfer fluctuation

The charge transfer fluctuation $\bar{D}_u(y)$ is qualitatively different than the net charge fluctuation $\delta Q^2(y_o)$. As will be shown in this section, the charge transfer fluctuation is capable of distinguishing the two phases of our two-component model and hence can be used as a signal for the QGP phase. In our model, the charge transfer fluctuation $\bar{D}_u(y)$ is given by

$$\bar{D}_u(y) = \frac{\delta Q^2(y_0)}{4} + 2\langle M_1\rangle \int_{-y_o}^{y} dy^- \int_{y}^{y_o} dy^+ f_1(y^+, y^-) + 2\langle M_2\rangle \int_{-y_o}^{y} dy^- \int_{y}^{y_o} dy^+ f_2(y^+, y^-), \quad (33)$$

and the final particle spectrum is

$$\frac{dN_{\rm ch}}{dy} = 2\langle M_1\rangle h_1(y) + 2\langle M_2\rangle h_2(y), \quad (34)$$

where $h_i(y) = \int_{-\infty}^{\infty} dx\, f_i(x, y)$.

For small γ_i, it is easy to show that

$$\bar{D}_u(y) \sim \text{constant} + \gamma_1\langle M_1\rangle F_1(y) + \gamma_2\langle_2\rangle F_2(y), \quad (35)$$

and the rapidity spectrum becomes

$$\frac{dN_{\rm ch}}{dy} \sim \langle M_1\rangle F_1(y) + \langle M_2\rangle F_2(y). \quad (36)$$

Hence, changes in the charge transfer fluctuation compared to the charged particle spectrum reflect changes in the concentration of the two components and/or the change in the mean correlation length. When the correlation lengths are not very small, $\bar{D}_u(y)$ is given in terms of the convolution of $F_1(y)$ and $F_2(y)$ with the corresponding relative distribution $R_1(r)$ and $R_2(r)$. Unless the γ's are very large, the ratio $\bar{D}_u(y)/(dN_{\rm ch}/dy)$ should still be sensitive to changes in the composition.

If the net charge fluctuation $\delta Q^2(y_o)$ is sizable, its presence can reduce the sensitivity of the ratio

$$\bar{\kappa}(y) = \frac{\bar{D}_u(y)}{(dN_{\rm ch}/dy)} \quad (37)$$

to the changing composition since $dN_{\rm ch}/dy$ abruptly decreases beyond the central plateau. However, since this $\delta Q^2(y_o)$ is the *uncorrected* net charge fluctuation, it is easy to measure and subtract it from $\bar{D}_u$. In this case, the relevant ratio becomes

$$\tilde{\kappa}(y) = \frac{\bar{D}_u(y) - \delta Q^2(y_o)/4}{(dN_{\rm ch}/dy)}. \quad (38)$$

If $dN_{\rm ch}/dy$ is flat within the observational window, this is of course not necessary as the $\delta Q^2(y_o)$ term just adds a constant. Also, in the large-y_o limit, $\delta Q^2(y_o) \to 0$ because of overall charge conservation and hence this modification is not necessary.

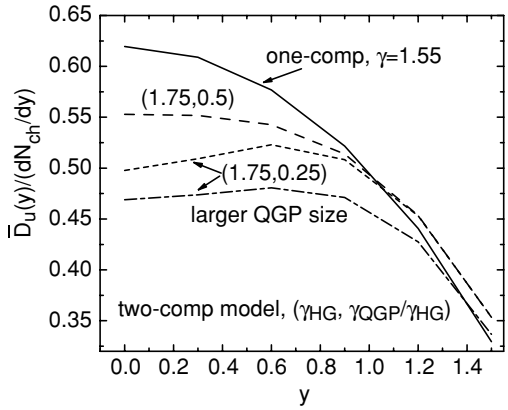

FIG. 11. The ratio of the charge transfer fluctuations to the total number of charges, $\bar{D}_u(y)/(dN_{\rm ch}/dy)$, in the rapidity observation window $(-1.5, 1.5)$ plotted as a function of the forward-backward separation cut y in the one-component and two-component models. For the one-component model, the charge correlation length is fixed at $\gamma = 1.55$. For the two-component models, the pair of correlation lengths $(\gamma_{\rm HG}, \gamma_{\rm QGP}/\gamma_{\rm HG})$ are labeled on each line. For the middle two lines, the QGP sizes ξ are fixed by requiring the net charge fluctuations to be constant at $\delta Q^2(0.5)/N_{\rm ch}(0.5) = 0.85$. The two lines with the same charge correlation lengths $(\gamma_{\rm HG}, \gamma_{\rm QGP}/\gamma_{\rm HG}) = (1.75, 0.25)$ have different QGP size.

The quantities $\bar{\kappa}(y)$ within $-1.5 < y < 1.5$ are plotted in Fig. 11 as a function of the forward-backward rapidity separation y in the one- and two-component models. In reality, the extreme peripheral collisions and the central collisions are candidates for the one- and two-component models, respectively. Because our $dN_{\rm ch}/dy$ is almost flat within this window, we do not need to subtract the $\delta Q^2(y_o)$ part. The shape for the one-component model is completely fixed by the charge correlation length $\gamma = 1.55$ as before, and it is a decreasing function of y. For the dashed and the dotted lines, we use the same parameters as obtained in the last section based on the experimentally observed net charge fluctuations. Even though the one- and two-component cases have a common net charge fluctuation at $y_o = 0.5$, the charge transfer fluctuation patterns are quite different: The most prominent feature for the two component model is the appearance of the minimum for $\bar{\kappa}(y)$ at $y = 0$ for $\gamma_{\rm QGP} < 0.5\gamma_{\rm HG}$, whereas the single-component case always has a maximum at $y = 0$.

The minimum appears at midrapidity because that is where the QGP component is concentrated. As y increases, the fraction of QGP matter decreases. Hence, $\bar{\kappa}(y)$ increases as a function of $y > 0$. The point where the slope of $\bar{\kappa}(y)$ changes sign must be directly related to the width of the QGP component. Unfortunately, when the size of the observation window and the width of the QGP component are similar, the sensitivity to the size of the QGP component is partially lost because $\bar{\kappa}(y)$ must decrease as y approaches the edge. To measure the size of the QGP component well, one needs to have $y_o \gg \xi$. This prompts us to extend the rapidity window of our observation in the two-component calculations.

In Fig. 12, we plot $\bar{\kappa}(y)$ with two different ξ's as a function of y. The observation window used is $(-6.0, 6.0)$, which is large compared to the size of the QGP component. One can

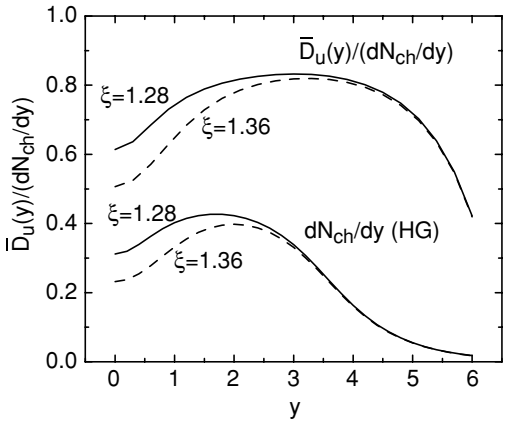

FIG. 12. The charge transfer fluctuations $\bar{D}_u(y)/(dN_{\rm ch}/dy)$ shown as a function of the forward-backward rapidity cut y in the two-component system. The QGP size is indicated by the parameter ξ. We have also plotted the corresponding hadron gas charge profiles, $dN_{\rm ch}/dy$(HG), for the two sets of calculations.

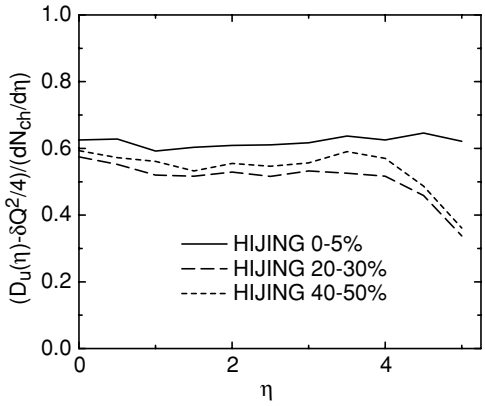

FIG. 13. A plot of ratios $(D_u(\eta) - \delta Q^2/4)/(dN_{\rm ch}/d\eta)$ for three different centrality classes using 50,000 minimum-bias HIJING events for Au-Au collisions at $\sqrt{s} = 200\,\text{GeV}$.

conclude that the width of the depression around midrapidity does reflect the width of the QGP component. A nearly flat $\bar{\kappa}(y)$ for $y > |\xi|$ is expected since in this region we should recover the single-component result. The decrease near the edge is again due to the finite window size. Also shown are the shapes of the HG contribution to the rapidity spectrum as a reference. The charge transfer fluctuations with the same two ξ's as before are also shown in Fig. 11. In the case of a more limited window, sensitivity to the size of the QGP component is reduced because the size of $y_{\rm o}$ is in fact about the same as the width of the QGP part ξ.

The charge transfer fluctuation $\bar{D}_u(y)$ is completely different from the net charge fluctuation $\delta Q^2(y_{\rm o})$ as far as the observation window size effect is concerned. As discussed before, having a larger observation window cannot increase the sensitivity of the net charge fluctuations to the QGP phase when it is confined to a small region around midrapidity. However, for charge transfer fluctuations, having a large observation window increases the sensitivity since the window now encompasses more of the QGP part. Enlarging the observation window also reduces the edge effect, increasing the sensitivity even more. An additional advantage for the charge transfer fluctuations is that there is no global charge conservation correction, unlike for the net charge transfer fluctuations.

For further reference, we show the result of analyzing 50,000 minimum-bias HIJING events for Au-Au collisions at $\sqrt{s} = 200\,\text{GeV}$ in Fig. 13 for three different centrality classes. Again the analysis is carried out in pseudorapidity space. The data points used are the same as in Fig. 4 except that the charge transfer fluctuations are corrected for the overall net charge fluctuations as in Eq. (38). The fact that $\delta Q^2 \neq 0$ even in full phase space is due to the spectators. Since the net charge carried by spectator nucleons fluctuates, so does the net charge of the produced particles. In the usual way of characterizing the centrality classes (by $N_{\rm ch}$ or E_T), this is unavoidable. It should be observed that for all centrality classes, the ratio $\bar{\kappa}(\eta) = (D_u(\eta) - \delta Q^2/4)/(dN_{\rm ch}/d\eta)$ is essentially flat. It is somewhat surprising that the Thomas-Chao-Quigg relationship works well for HIJING events given the fact that no "cluster" appears explicitly within HIJING.

The two-component model discussed here is admittedly a best-case scenario. It is possible that the reduced net charge fluctuations from QGP are realized by some mechanism other than neutral-cluster formation. In that case, the charge correlation length does not have to be smaller than the hadronic one and $\kappa(y)$ will not have a minimum.

One possible concern is the effect of kinetic focusing caused by the radial flow. If the charge correlation length is significantly reduced by the strong radial flow at midrapidity, one may also observe a minimum at the center. Fortunately, this is not the case for RHIC energy reactions. By calculating the momentum changes of the correlated pion pairs resulting from the flow, we find that the change of (pseudo)rapidity charge correlation length is less than 2%.

C. Forward-backward multiplicity correlation

The key points in our discussion thus far are as follows: (i) There are primordial clusters that produce multiple particles, (ii) a local cut separates the phase space into two regions, and (iii) one can define observables that only count the primordial clusters that have their decay products separated by the local cut (cf. Fig. 1). These points imply that such observables are sensitive to the local properties around the cut. Hence, if the nature of the "clusters" changes in different regions of the phase space, then these observables can detect the changes.

In some experiments, such as PHOBOS at RHIC, charge states of the produced particles cannot be determined. In this case, charge transfer fluctuation cannot be used. However, since the essence of the current method is to have a cut that separates produced particles, just measuring the forward-backward multiplicity correlation,

$$w(\eta) = \langle N_F(\eta) N_B(\eta)\rangle - \langle N_F(\eta)\rangle\langle N_B(\eta)\rangle, \qquad (39)$$

may be enough to detect the change in correlation length. Here $N_F(\eta)$ is the charged multiplicity in the region forward of the pseudorapidity η and $N_B(\eta)$ is the charged multiplicity in the region backward of η. This is a slight variation of

the charge transfer fluctuations and was also studied in early *NN* reactions [55–57].

In this section, we switch to the pseudorapidity η since without particle identification one cannot determine the rapidity y. However, in the current formulation of the problem, the only change this switch introduces is that instead of rapidity correlation function $f_i(y, y')$ we have the pseudorapidity correlation function $f_i(\eta, \eta')$.

Using the two-component model [Eq. (27)], one can show that

$$\begin{aligned} w(\eta) = {} & 4\left(\left\langle \delta M_1^2 \right\rangle - \langle M_1 \rangle\right) \int_{\eta}^{\eta_o} d\eta\, h_1(\eta) \int_{-\eta_o}^{\eta} d\eta\, h_1(\eta) \\ & + 4\left(\left\langle \delta M_2^2 \right\rangle - \langle M_2 \rangle\right) \int_{\eta}^{\eta_o} d\eta\, h_2(\eta) \int_{-\eta_o}^{\eta} d\eta\, h_2(\eta) \\ & + 2\langle M_1 \rangle \int_{\eta}^{\eta_o} d\eta' \int_{-\eta_o}^{\eta} d\eta''\, f_1(\eta', \eta'') \\ & + 2\langle M_2 \rangle \int_{\eta}^{\eta_o} d\eta' \int_{-\eta_o}^{\eta} d\eta''\, f_2(\eta', \eta''), \end{aligned} \tag{40}$$

where the correlation functions f_1 and f_2 are functions of pseudorapidities and we defined

$$h_i(\eta) = \int_{-\infty}^{\infty} d\eta'\, f_i(\eta', \eta). \tag{41}$$

The nontrivial part of this expression is essentially the same as the charge transfer fluctuations. The sensitivity of this observable to changes in the pseudorapidity correlation length depends crucially on the size of the first two terms containing $\langle \delta M_i^2 \rangle - \langle M_i \rangle$. If the number fluctuations of the clusters obey Poisson statistics, then these two terms vanish. In that case, $w(\eta)$ is as sensitive as the charge transfer fluctuation to the presence of the second phase. In the limit where there is only a single species of clusters and also $\eta_o \to \infty$, we have an additional Thomas-Chao-Quigg relationship

$$w(\eta) \approx \kappa \frac{dN_{\rm ch}}{d\eta}, \tag{42}$$

with a constant κ, provided that $\langle \delta M^2 \rangle = \langle M \rangle$.

The ratio of the forward-backward multiplicity correlation $w(\eta)$ to the charged particle yield $dN_{\rm ch}/d\eta$ is plotted in Fig. 14. When the clusters are distributed according to Poisson distributions, the Thomas-Chao-Quigg relationship holds for a single-component model and the ratio of $w(\eta)/(dN_{\rm ch}/d\eta)$ is flat in the central region (the solid line in Fig. 14). For a two-component model with Poisson statistics (long dashed line), we see a minimum at midrapidity just as in the charge transfer fluctuation.

When the statistics deviate from Poisson, the factor $\langle \delta M_i^2 \rangle - \langle M_i \rangle$ is nonzero. Then the first two terms in Eq. (40) contributes. These terms decrease with η and hence partially compensate the rising part that results from the correlation change. However, the qualitative trend of the forward-backward multiplicity correlation remains valid: The local minimum is still present in the two-component model and is an indication of the presence of a QGP.

For heavy particles originating from a thermally equilibrated system, the multiplicity fluctuation should follow

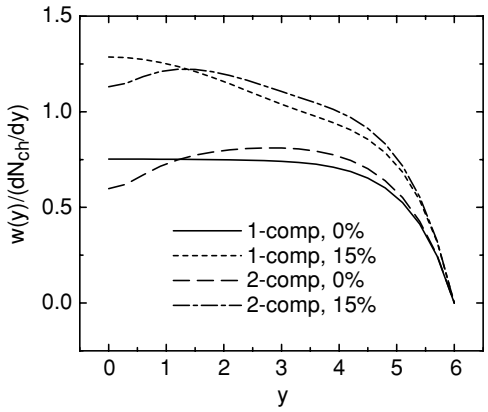

FIG. 14. The ratio of the forward-backward multiplicity correlation $w(\eta)$ to the charged particle yield $dN_{\rm ch}/d\eta$ plotted as a function of η for one-component and two-component models. The fluctuations of the total number of charged particles are also indicated for the corresponding lines. The distribution of M_i ($i = 1$ or 2), deviates from a Poisson distribution by 0%, that is, $\langle \delta M_i^2 \rangle - \langle M_i \rangle = 0$. We have also included the results for 15% deviations.

Poisson statistics. For light particles, $\langle \delta M^2 \rangle$ can deviate up to 15% from the Poisson value. As an estimate, in Fig. 14 we show our results with $\langle \delta M_i^2 \rangle - \langle M_i \rangle = 0.15\,\langle M_i \rangle$. One can still see a clear dip near midrapidity.

Coincidentally, the PHOBOS group has also measured a variation of the signal we proposed here (see Ref. [53]). The difference between the forward-backward multiplicity correlation $w(\eta)$ and the "charged particle multiplicity fluctuations" $\sigma(C)$ used by the PHOBOS group is subtle but results in quite different sensitivity. The signal $\sigma(C)$ in Ref. [53] measures the correlations between rapidity regions of $(-\eta - \Delta\eta/2, -\eta + \Delta\eta/2)$ and $(\eta - \Delta\eta/2, \eta + \Delta\eta/2)$, with each region covering the same rapidity window of $\Delta\eta = 0.5$, 1.0, and 1.5. Typically these two rapidity regions do not have a common edge. In our case, the two pseudorapidity regions are $(-\eta_o, \eta)$ and (η, η_o). They share a common edge at η, but the two regions are generally of different size. In the case where the two regions are separated, the multiplicity correlations measure the "long-range correlations" [58–60]. Where the two regions share a common edge, the correlations measure the "short-range correlations," as we have shown in this paper. For the special case of $\eta = \Delta\eta/2$ in the PHOBOS study, $\sigma(C)$ is the same as the forward-backward multiplicity correlation $w(0)$ as we proposed here. However, as we have shown in this paper, a point in the fluctuation measurement cannot distinguish between one-component and two-component models because the charge correlation length can be adjusted to fit this single point. One must measure $w(\eta)$ as a function of η to get full information on possible phase change.

V. SUMMARY

In this paper, we proposed charge transfer fluctuations as a signal for the QGP phase of matter. The essence of our argument is very simple. Suppose there are strong unlike-sign correlations in the underlying system, then the charges are locally conserved. With a separating wall in the local region

where we want to explore, the correlations (or fluctuations) of charges across this wall are sensitive to the *local* charge correlation length. The pairs created far away from the separating wall contribute little to the fluctuations since they have little chance of being separated by the wall. This is essentially the idea behind the charge transfer fluctuations proposed for earlier *pp* collisions.

Since the charge transfer fluctuation $D_u(y)$ is a local measure of the unlike-sign correlation length, it can be used to detect the presence of a second phase in *AA* collisions. Quite generally, one can say that the presence of a local *minimum* at $y = 0$ for the ratio $\kappa(y) = D_u(y)/(dN_{\rm ch}/dy)$ is a signal for the second (presumably QGP) phase. This minimum appears because (i) a QGP phase should appear around midrapidity where the density is the highest and (ii) hadrons coming out of a QGP phase should have a markedly short unlike-sign correlation length compared to that of the hadronic matter. The size of the depression near midrapidity in turn contains information on the size of the QGP phase. If one has a large observation window, the extent of the second phase in the rapidity space can be in fact estimated by the width of the dip.

Extending the idea of charge transfer fluctuations, we also proposed the forward-backward multiplicity correlation as a possible signal for the presence of a QGP. A case study with a few hadronic event generators is under way.

ACKNOWLEDGMENTS

The authors thank C. Gale, V. Topor Pop, V. Koch, and G. Westfall for stimulating discussions and J. Barrette for his critical reading of the manuscript. S. J. is supported in part by the Natural Sciences and Engineering Research Council of Canada and by le Fonds Nature et Technologies of Québec. S. J. also thanks the RIKEN BNL Center and the U.S. Department of Energy (DE-AC02-98CH10886) for providing facilities essential for the completion of this work.

APPENDIX A: EFFECT OF NET POSITIVE CHARGES

For the uncorrelated charged particles in the system, keeping the total charge constant in the system, we find the charge transfer fluctuations to be

$$\bar{D}_u(y) = \frac{\langle M_{\rm ch}\rangle}{4}\int_{-y_{\rm o}}^{y_{\rm o}} dy' g(y') - \frac{\langle M_{\rm ch}\rangle}{4}\left(\int_{y}^{y_{\rm o}} dy' g(y') - \int_{-y_{\rm o}}^{y} dy' g(y')\right)^2. \quad \text{(A1)}$$

In deriving this result, we have assumed that the positive and negative charges have the same normalized distribution, $g(y)$. Otherwise, we have to count the contributions from both positive and negative charges separately in Eq. (A1), and additionally there will be an extra term corresponding to the difference of the positive and negative charge forward-backward asymmetry.

The first term in Eq. (A1) comes from the overall fluctuations of charged particle number in the observation window and its value is the same as in the net charge fluctuations case (except for a factor of 4). The second term is due to the forward-backward asymmetry in the charge transfer definition. In the limit that the observation window is sufficiently large, Eq. (A1) reduces to the second integral in Eq. (7).

In the case that the system has both uncorrelated charges and correlated charges, we only need to add the result in Eq. (A1) to the previous result for correlated charges, Eq. (25). This will not change the quantitative features of the charge transfer fluctuations as a function of rapidity. The first term in Eq. (A1) is independent of y and will not affect any of our discussion except by adding a constant. The second term is a decreasing function of y. Therefore, the contribution from uncorrelated charges is still a decreasing function of the forward-backward rapidity cut y. This is in line with the results for correlated charges. The decreasing trend of the charge transfer fluctuations as a function of the forward-backward rapidity cut y in a uniform system is unchanged by this additional contribution. The existence of a local minimum will still be a signal of a second phase with smaller charge correlation length.

Since in realistic heavy-ion collisions at RHIC energies most positive and negative charges are created together with an opposite charge to conserve net total charge, we can safely assume that uncorrelated charges are rare. The net positively charged particles originating from the projectile and the targets is only a small fraction of the total number of charged particles in RHIC energy heavy-ion collisions. For this reason, the corrections from uncorrelated charges are ignored in most of this study. The qualitative features of the charge transfer fluctuations will not be sensitive to this correction term.

We can make a simple estimate of the corrections from these uncorrelated charges by assuming the uncorrelated charges are from the protons in the initial collision system. The maximum of the second term in Eq. (A1) scales as $p^2 M_+/M_0$, where p is the fraction of observed uncorrelated charges to the total number of uncorrelated charges. In RHIC energy heavy-ion reactions, $M_+/M_0 \sim 0.04$ and p is typically around 5% in the central region. Indeed, the corrections from uncorrelated charges is quite small, of order 10^{-4}. The corrections to the net charge fluctuations from the uncorrelated charges are of the same order of magnitude as the corrections to the charge transfer fluctuations. The net charge fluctuations $D_c(y_{\rm o})$ and the total number of charges $N_{\rm ch}(y_{\rm o})$ both acquire additional terms and they are both equal to four times the first term in Eq. (A1).

APPENDIX B: NONZERO CHARGE TRANSFER CASE

When the charge transfer $u(y)$ in Eq. (3) does not average to zero, the charge transfer fluctuations will acquire additional terms that are quadratic to the average charge transfer.

In the neutral-cluster model, the full result for the charge transfer fluctuations is

$$\bar{D}_u(y) = \frac{\langle M_0\rangle}{2}(W_L + W_R + 2W_y) + \frac{\langle u(y)\rangle^2}{\langle M_0\rangle^2}\left(\langle \delta M_0^2\rangle - \langle M_0\rangle\right). \quad \text{(B1)}$$

The weights for left and right edges of the observation window $(-y_{\rm o}, y_{\rm o})$ and for the forward-backward rapidity cut y

are defined as

$$W_L = \int_{-\infty}^{-y_o} dy' \int_{-y_o}^{y_o} dy'',\, f_0(y', y''),$$
$$W_R = \int_{-y_o}^{y_o} dy' \int_{y_o}^{\infty} dy'',\, f_0(y', y''), \tag{B2}$$
$$W_y = \int_{-y_o}^{y} dy' \int_{y}^{y_o} dy''\, f_0(y', y'').$$

The last term in Eq. (B1) stems from the nonzero average charge transfer in the system. An estimate would give $\langle u(y)\rangle \leqslant 10$ and $\langle \delta M_0^2\rangle - \langle M_0\rangle \sim 0.1 M_0$, and the error from neglecting this nonzero average charge transfer is typically less than 10^{-5}.

APPENDIX C: SOLUTION OF EQ. (11)

The Thomas-Chao-Quigg equation for the neutral-cluster distribution function is given by

$$\int_{-\infty}^{z} dy \int_{z}^{\infty} dx\; f_0(x, y) = \kappa \int_{-\infty}^{\infty} dy\; f_0(y, z). \tag{C1}$$

We make the following ansatz:

$$f_0(x, y) = g(r)F(Y), \tag{C2}$$

where $r = x - y$ and $Y = (x + y)/2$ and with $g(-r) = g(r)$. Changing variables to r and Y, we rewrite Eq. (C1) as

$$\int_0^{\infty} dr\; g(r) \int_{z-r/2}^{z+r/2} dY\; F(Y) = \kappa \int_{-\infty}^{\infty} dr\; g(r) F(z + r/2). \tag{C3}$$

We can now Taylor-expand both $\int_{z-r/2}^{z+r/2} dY\, F(Y)$ and $F(z + r/2)$ with respect to r and get the following relationship between the moments of $g(r)$:

$$R_{2n+1}/R_{2n} = 2\kappa(2n + 1), \tag{C4}$$

where

$$R_s \equiv \int_0^{\infty} dr\; g(r) r^s \tag{C5}$$

and we used the fact that $g(r)$ is an even function.

Note that

$$\int_0^{\infty} dx\; e^{-x/2\kappa} x^n = 2^{n+1}\kappa^{n+1} n! \tag{C6}$$

so that

$$\frac{\int_0^{\infty} dx\; e^{-x/2\kappa} x^{2n+1}}{\int_0^{\infty} dx\; e^{-x/2\kappa} x^{2n}} = \frac{2^{2n+2}\kappa^{2n+2}(2n + 1)!}{2^{2n+1}\kappa^{2n+1}(2n)!} = 2\kappa(2n + 1). \tag{C7}$$

Therefore

$$g(r) = C \exp(-|r|/2\kappa), \tag{C8}$$

where C is a normalization constant. Hence, the solution of Eq. (11) is given by

$$f_0(x, y) = \mathcal{N} \exp(-|x - y|/2\kappa) F((x + y)/2), \tag{C9}$$

where $F(Y)$ can be quite arbitrary as long as its derivatives are all finite and the integrals in Eq. (11) are well defined.

[1] K. Adcox *et al*. (PHENIX), Nucl. Phys. **A757**, 184 (2005).
[2] B. B. Back *et al*. (PHOBOS), Nucl. Phys. **A757**, 28 (2005).
[3] J. Adams *et al*. (STAR), Nucl. Phys. **A757**, 102 (2005).
[4] I. Arsene *et al*. (BRAHMS), Nucl. Phys. **A757**, 1 (2005).
[5] E. V. Shuryak, Nucl. Phys. **A750**, 64 (2005).
[6] J.-P. Blaizot and E. Iancu, Phys. Rep. **359**, 355 (2002).
[7] E. Iancu, A. Leonidov, and L. D. McLerran, Nucl. Phys. **A692**, 583 (2001).
[8] E. Ferreiro, E. Iancu, A. Leonidov, and L. McLerran, Nucl. Phys. **A703**, 489 (2002).
[9] J.-P. Blaizot and E. Iancu, Nucl. Phys. **B557**, 183 (1999).
[10] X.-N. Wang and M. Gyulassy, Phys. Rev. D **44**, 3501 (1991).
[11] X.-N. Wang and M. Gyulassy, Phys. Rev. D **45**, 844 (1992).
[12] M. Gyulassy and X.-N. Wang, Comput. Phys. Commun. **83**, 307 (1994).
[13] X.-N. Wang, Phys. Rep. **280**, 287 (1997).
[14] H. Sorge, Z. Phys. C **67**, 479 (1995).
[15] H. Sorge, Phys. Rev. C **52**, 3291 (1995).
[16] S. A. Bass *et al*., Prog. Part. Nucl. Phys. **41**, 225 (1998).
[17] M. Bleicher *et al*., J. Phys. G **25**, 1859 (1999).
[18] C. Gale and J. Kapusta, Phys. Rev. C **35**, 2107 (1987).
[19] Z.-W. Lin, C. M. Ko, and S. Pal, Phys. Rev. Lett. **89**, 152301 (2002).
[20] C. Quigg and G. H. Thomas, Phys. Rev. D **7**, 2752 (1973).
[21] A. W. Chao and C. Quigg, Phys. Rev. D **9**, 2016 (1974).
[22] T. Kafka *et al*., Phys. Rev. Lett. **34**, 687 (1975).
[23] S. A. Bass, P. Danielewicz, and S. Pratt, Phys. Rev. Lett. **85**, 2689 (2000).
[24] V. Koch, M. Bleicher, and S. Jeon, Nucl. Phys. **A698**, 261 (2002).
[25] E. V. Shuryak, Phys. Lett. **B423**, 9 (1998).
[26] M. A. Stephanov, K. Rajagopal, and E. Shuryak, Phys. Rev. D **60**, 114028 (1999).
[27] S. Mrowczynski, Phys. Lett. **B465**, 8 (1999).
[28] R. Korus and S. Mrowczynski, Phys. Rev. C **64**, 054906 (2001).
[29] L. Stodolsky, Phys. Rev. Lett. **75**, 1044 (1995).
[30] M. Asakawa, U. Heinz, and B. Muller, Phys. Rev. Lett. **85**, 2072 (2000).
[31] S. Jeon and V. Koch, Phys. Rev. Lett. **85**, 2076 (2000).
[32] J. T. Mitchell, J. Phys. G **30**, S819 (2004).
[33] S. J. Lindenbaum and R. S. Longacre, BNL Report 52636 (unpublished), nucl-th/0108061.
[34] K. Adcox *et al*. (PHENIX), Phys. Rev. Lett. **89**, 082301 (2002).
[35] J. Adams *et al*. (STAR), Phys. Rev. C **68**, 044905 (2003).
[36] C. A. Pruneau (STAR), Poster presented at Quark Matter 2004, nucl-ex/0401016.
[37] J. Nystrand, E. Stenlund, and H. Tydesjo, Phys. Rev. C **68**, 034902 (2003).
[38] S. Jeon and S. Pratt, Phys. Rev. C **65**, 044902 (2002).
[39] S. Cheng *et al*., Phys. Rev. C **69**, 054906 (2004).
[40] J. Adams *et al*. (STAR), Phys. Rev. Lett. **90**, 172301 (2003).

[41] M. B. Tonjes, Ph.D. thesis, Michigan State University, 2002.
[42] G. D. Westfall (STAR), J. Phys. G **30**, S345 (2004).
[43] J. D. Bjorken, Phys. Rev. D **27**, 140 (1983).
[44] B. B. Back *et al*. (PHOBOS), Phys. Rev. C **65**, 031901(R) (2002).
[45] B. B. Back *et al*. (PHOBOS), Phys. Rev. C **70**, 061901(R) (2004).
[46] I. G. Bearden *et al*. (BRAHMS), Phys. Rev. Lett. **94**, 162301 (2005).
[47] J. Adams *et al*. (STAR), nucl-ex/0311017.
[48] B. B. Back *et al*. (PHOBOS), nucl-ex/0407012.
[49] C. Pruneau, S. Gavin, and S. Voloshin, Phys. Rev. C **66**, 044904 (2002).
[50] S. Jeon and V. Koch, Phys. Rev. Lett. **83**, 5435 (1999).
[51] E. L. Berger, D. Horn, and G. H. Thomas, Phys. Rev. D **7**, 1412 (1973).
[52] V. Topor Pop, M. Gyulassy, J. Barrette, C. Gale, X.-N. Wang, N. Xu, and K. Filimonov, Phys. Rev. C **68**, 054902 (2003).
[53] K. Wozniak *et al*. (PHOBOS), J. Phys. G **30**, S1377 (2004).
[54] K. Fialkowski and R. Wit, Europhys. Lett. **55**, 184 (2001).
[55] T. Ludlam and R. Slansky, Phys. Rev. D **12**, 59 (1975).
[56] H. Braun *et al*., Phys. Rev. D **17**, 1260 (1978).
[57] T. T. Chou and C. N. Yang, Phys. Rev. D **7**, 1425 (1973).
[58] N. S. Amelin, N. Armesto, M. A. Braun, E. G. Ferreiro, and C. Pajares, Phys. Rev. Lett. **73**, 2813 (1994).
[59] M. A. Braun, R. S. Kolevatov, C. Pajares, and V. V. Vechernin, Eur. Phys. J. C **32**, 535 (2004).
[60] M. A. Braun and C. Pajares, Eur. Phys. J. C **16**, 349 (2000).